Published version available at https://doi.org/10.1007/s00027-020-0708-2

# Title: **Diel cycles of $\delta^{13}C_{DIC}$ and ecosystem metabolism in ephemeral dryland streams**

Authors: Andre R. Siebers[1,2,*], Neil E. Pettit[1,3], Grzegorz Skrzypek[1], Shawan Dogramaci[1,4], Pauline F. Grierson[1]

[1]Ecosystems Research Group and West Australian Biogeochemistry Centre, School of Biological Sciences, The University of Western Australia, 35 Stirling Highway, Crawley, WA 6009, Australia

[2]Current address: Department of Aquatic Ecology, Eawag – Swiss Federal Institute of Aquatic Sciences, Überlandstrasse 133, 8600 Dübendorf, Switzerland

[3]Centre of Excellence in Natural Resource Management, The University of Western Australia, 35 Stirling Terrace, Albany, WA 6332, Australia

[4]Rio Tinto Iron Ore, 152-158 St. Georges Terrace, Perth, WA 6000, Australia

[*]Corresponding author:

Email: andre.siebers@outlook.com

Address: c/o Eawag Eco, Überlandstrasse 133, 8600 Dübendorf, Switzerland.

Phone: +41 76 226 6144

ORC IDs:

A.R. Siebers: 0000-0002-8326-1649. N.E. Pettit: 0000-0001-6126-8914. G. Skrzypek: 0000-0002-5686-2393. S. Dogramaci: 0000-0002-2598-0442. P.F. Grierson: 0000-0003-2135-0272.

## Abstract

Streams in hot, arid environments often exist as a series of isolated pools along main channels. During these periods, shallow alluvial throughflow may strongly influence key ecological processes within pools. We measured diel changes in $\delta^{13}C$ values of dissolved inorganic carbon (DIC) and dissolved oxygen (DO) in two pools of ephemeral, dryland streams. We quantified alluvial water connectivity through stable isotope analysis ($\delta^{18}O$ and $\delta^{2}H$) of pool and alluvial water. We also estimated gross primary productivity (GPP) and ecosystem respiration (ER) rates across a wider set of pools in both streams. $\delta^{13}C_{DIC}$ values displayed regular diel cycles, where both pools displayed small but similar daily amplitude (0.7 – 0.9‰) despite contrasting amplitudes of change in DO (0.8 mg $L^{-1}$ vs. 2.8 mg $L^{-1}$) and contrasting alluvial water connectivity (connected vs. disconnected). Water temperature was the strongest predictor of both $\delta^{13}C_{DIC}$ values and rates of change in $\delta^{13}C_{DIC}$ across both pools. Across both streams, all pools were net heterotrophic. GPP (0.35 to 1.73 g $O_2$ $m^{-2}$ $d^{-1}$) and ER (0.49 to 2.64 g $O_2$ $m^{-2}$ $d^{-1}$) rates were linked to aquatic vegetation cover. The disconnect between diurnal amplitudes of $\delta^{13}C$ values and DO concentrations thus suggests that ecological drivers of gas exchange became increasingly localised as pools contracted.



## Keywords

Dissolved inorganic carbon; alluvial water connectivity; intermittent streams; temperature; water isotopes

## Acknowledgements

Funding for this study was provided by an Australian Research Council linkage grant to The

University of Western Australia and Rio Tinto Iron Ore (LP0776626) and an Australian Research Council Future Fellowship awarded to Grzegorz Skrzypek (FT110100352). We thank Jordan Iles and Jennifer Kelley for access to unpublished data from subsequent samples from Coondiner Creek. The authors also wish to thank Kate Bowler and Doug Ford for laboratory assistance, and Grace Campbell, Romony Coyle, and Jennifer Kelley for assistance in the field. Our thanks to Chris Robinson and several anonymous reviewers who provided suggestions that greatly improved the quality of this article.

## Introduction

Rivers and streams in dryland regions often have ephemeral flow regimes, especially in highly seasonal, hot arid climates. Flow regimes in these regions are characterised by short, but intense flood events, followed by longer dry periods where surface water contracts into isolated pools along main channels (e.g., Capone and Kushlan, 1991, Bunn et al., 2003, Fellman et al., 2011, Vazquez et al., 2011, Siebers et al., 2016). While flow pulse cycles are recognised as vital to the biogeochemical cycles and productivity of dryland fluvial systems (Bunn et al., 2006b), the effects of drying on their functioning are poorly understood (Lake, 2003), in large part due to the complexity of interacting processes. For example, the lack of surface flow reduces physical disturbance of primary producers (macrophytes, biofilms). Gross primary productivity (GPP) can thus be high in dryland streams (e.g. Grimm and Fisher, 1986, 1989; Bunn et al., 2003, Fellows et al., 2009), releasing organic matter that then supports ecosystem respiration (ER) (Jones et al., 1995, Fellows et al., 2007, Townsend et al., 2011). Flow cessation also reduces hydrological connectivity between pools and the terrestrial environment. However, reaches with riparian woodland may have large inputs of leaf litter even through the dry season, with high retention due to the lack of surface flow (von Schiller et al., 2017). These leaf litter inputs represent a significant source of dissolved organic matter (DOM) (Casas-Ruiz et al., 2016) and can support substantial heterotrophic respiration (Acuña et al., 2004). The balance between GPP and ER might thus vary considerably as pools dry and contract (von Schiller et al., 2017).

Ecosystem metabolism (broadly defined as variation in GPP and ER; Odum 1956) in dryland streams might also be driven by the extent of connectivity to shallow alluvial groundwater (e.g. Dahm et al., 2003). Shallow alluvial inputs and hyporheic exchange can be important sources of limiting nutrients such as inorganic nitrogen (Valett et al., 1994), the uptake of

which is tightly coupled to ecosystem metabolism (Tank et al., 2017). During drying periods, GPP might thus increase due to inputs of inorganic nutrients from subsurface flowpaths (Fisher et al., 1998a, Dahm et al., 2003). In dryland regions, shallow alluvial inputs may further promote autotrophic processes through relatively high inorganic:organic nutrient ratios caused by low dissolved organic matter (DOM) concentrations within sub-surface flows (e.g. Valett et al., 1996, Dahm et al., 2003, Vazquez et al., 2011). Alluvial water connectivity might further alleviate evaporative contraction of pools (Siebers et al., 2016), reducing the loss of aquatic plants and algae along drying fronts (Stanley et al., 1997). GPP might be thus higher in reaches with shallow alluvial water connectivity. However, alluvial water connectivity might also increase ER rates. DOM in the shallow, alluvial groundwater of dryland streams can be highly labile and rapidly mineralised at the sediment-water interface (Jones, 2002, Fellman et al., 2014). Increasing GPP rates might also support higher ER rates, particularly if GPP results in the production of relatively labile algal organic matter (Mulholland et al., 2001, Townsend et al., 2011). Consequently, reaches with connectivity to alluvial flowpaths likely have higher daily rates of both GPP and ER when compared to those without sub-surface connectivity.

Although dissolved oxygen (DO) is the most widely used tracer of ecosystem metabolism in aquatic systems (Demars et al. 2015), daily dynamics of dissolved inorganic carbon (DIC; including $CO_2$, $HCO_3^-$ and $CO_3^{2-}$) also are reactants in ecosystem metabolism. In freshwater systems, diel variation in DIC is strongly driven by the uptake of aqueous $CO_2$ or $HCO_3^-$ by photosynthetic organisms during the day. Production of $CO_2$ by respiration conversely increases DIC concentrations at night (Nimick et al., 2011). However, DIC is also strongly affected by physical and chemical processes. Groundwater flowpaths often have high concentrations of $CO_2$ and $HCO_3^-$, which can supersaturate surface waters and result in high

rates of $CO_2$ outgassing (Cole et al., 2007, Battin et al., 2008, Hotchkiss et al., 2015). Production and removal of $CO_2$ from the water column also affects pH, chemical speciation, and mineral precipitation and dissolution (Nimick et al., 2011). In addition, anaerobic carbon metabolism, particularly methanogenesis and methane oxidation, can contribute to variation in DIC (Bastviken et al., 2008). Considering DO and DIC cycles in parallel will aid in disentagling the complex effects of groundwater connectivity on ecosystem metabolism (e.g. Tobias and Böhlke, 2011).

The stable isotopic composition of DIC ($\delta^{13}C_{DIC}$) is a widely used tracer of DIC dynamics (Campeau et al., 2017). Average $\delta^{13}C_{DIC}$ values typically reflect a balance between biogenic DIC sources (ca. -30 to -20 ‰) and geological sources (ca. -12 ‰) (Finlay, 2003, Campeau et al. 2017). Invasion of atmospheric $CO_2$ (ca. -8.2 ‰; Keeling et al., 2010) can also affect $\delta^{13}C_{DIC}$, but is usually only significant in waters with low DIC concentrations. $\delta^{13}C_{DIC}$ values can then vary further due to local biogeochemical processes. First, DIC is strongly enriched in $^{13}C$ by photosynthetic fractionation (Farquhar et al. 1989). $CO_2$ outgassing also increases $\delta^{13}C_{DIC}$ values, both directly and through fractionation effects in the chemical equilibrium of DIC (Drysdale et al., 2003, Doctor et al., 2008, Tobias and Böhlke, 2011). Conversely, mineralization of organic matter typically reduces $\delta^{13}C_{DIC}$ values due to production of $CO_2$ with values reflecting highly $^{13}C$-depleted organic matter sources (Finlay, 2003). Anaerobic metabolism has contrasting effects on $\delta^{13}C_{DIC}$ values, as methanogenesis lowers $\delta^{13}C_{DIC}$ values while methane oxidation raises $\delta^{13}C_{DIC}$ (Campeau et al., 2017). However, relative to GPP and ER, most of these processes should occur at lower rates or do not have pronounced diurnal cycles. Consequently, diel variation in $\delta^{13}C_{DIC}$ should mostly be driven by ecosystem metabolism, with correlation between diel amplitude in $\delta^{13}C_{DIC}$ values and dissolved oxygen concentrations (Parker et al. 2005, 2010).

Here, we examined daily cycles of dissolved oxygen (DO) and $\delta^{13}C_{DIC}$ within two contrasting pools of ephemeral dryland streams during the drying period. One pool has relatively consistent connectivity to shallow alluvial groundwater while the other is typically disconnected from sub-surface flow (Siebers et al. 2016). To provide a more general landscape context of our results, we also measured rates of ecosystem metabolism (GPP and ER) across a greater set of pools within both streams. We aimed to establish whether i) measuring DO and $\delta^{13}C_{DIC}$ together allows us to quantify the effect of alluvial water connectivity on diurnal rates of GPP or ER, and ii) whether alluvial water connectivity might drive variation in GPP and ER rates more generally across these dryland pools.

## Material and methods

### *Study sites and sampling design*

The study was conducted at Coondiner Creek and Weeli Wolli Creek in separate catchments of the semi-arid Pilbara region, northwest Australia (Fig. 1). The area receives on average 300 – 350 mm annual rainfall, mostly during cyclonic events in the wet season (December-March; see Rouillard et al., 2015). In contrast, mean annual evaporation is ca. 3000 mm (Australian Bureau of Meteorology). Most streams are therefore ephemeral and usually only flow (typically, order of days) during heavy rainfall, subsequently drying into disconnected pools along main channels. Study reaches of both streams are characterised by clay-rich gravel beds along deeply incised channels (up to ca. 30 m). Despite the high clay content, alluvial sediments are loosely consolidated and shallow groundwater can exchange with surface water pools (Fellman et al., 2011, Dogramaci et al., 2012). Catchment geology is mostly banded-iron formations, mudstone, and siltstone, although channels dissect extensive calcrete surfaces in places, Weeli Wolli Creek in particular (Dogramaci et al., 2015). Both

streams were sampled during an inter-flood dry period around 9 months after the last major rainfall event, Cyclone Heidi (10-13 January 2012).

The Pilbara region is remote (ca. 1200 km from Perth, Australia), vast (ca. 500,000 $km^2$), and sparsely populated. Importantly, most streams in the region are unimpacted by anthropogenic stressors, making them excellent systems for studying functional processes of dryland waters. Due to the remote setting, we were able to obtain complete diel measures of the stable isotope composition of water ($\delta^{18}O$ and $\delta^{2}H$) and dissolved inorganic carbon ($\delta^{13}C_{DIC}$), as well as inorganic nutrient concentrations in just one pool in each stream. In Coondiner, the pool was located in a lower reach of a relatively well-studied section along the main channel (pool 3 in Fellman et al., 2011; here referred as CND3). In Weeli Wolli, we used the largest pool in a series of pools colloquially known as Ben's Oasis (here, BO3). Detailed sampling of Ben's Oasis is essentially lacking, but anecdotal evidence indicated the pools persist during dry periods. CND3 was sampled during 20-21 October 2012 and BO3 during 16-17 November 2012. Climatic conditions during sampling were hot (26°C at night, 42°C in early afternoon) and mostly clear, with no rainfall recorded.

In addition, we monitored diel cycles of dissolved oxygen at 3 other pools at Coondiner (CND1, 3, and 4 from 19-21 October 2012; Pools 1, 3, and 4 in Fellman et al., 2011) and 2 pools at Ben's Oasis (BO3, BO4 from 15-17 November 2012). Other studies of stable isotopic composition ($\delta^{18}O$ and $\delta^{2}H$) of ground water, rainfall, and surface water across the Pilbara indicated the pools to differ substantially in connectivity to throughflow of shallow alluvial water (i.e., groundwater inputs) and evaporation rates (Fellman et al., 2011, Dogramaci et al., 2012, Siebers et al., 2016). All pools were measured for $\delta^{18}O$ and $\delta^{2}H$, water chemistry, and habitat mapping (see below).

Briefly, $\delta^{18}O$ and $\delta^{2}H$ of pool water reflects local evaporation rates, humidity, rainfall amount and mixing of water sources (Gat, 1996). In the Pilbara, both surface water and alluvial groundwater are derived primarily from infrequent large rainfall events that have highly depleted $\delta^{18}O$ and $\delta^{2}H$ signatures (e.g. Skrzypek et al., 2013). Smaller rainfall events do not usually affect water budgets (Dogramaci et al., 2012). Pools in losing reaches thus exhibit predictable and linear increases in $\delta^{18}O$ and $\delta^{2}H$ values, while those connected to alluvial water reflect $\delta^{18}O$ and $\delta^{2}H$ values of that alluvial groundwater (Fellman et al., 2011, Dogramaci et al., 2012). The local evaporation line (relationship describing variation in $\delta^{18}O$ and $\delta^{2}H$ under local evaporation conditions) for both catchments was significantly different from the local meteoric water line (relationship between $\delta^{18}O$ and $\delta^{2}H$ in local precipitation; Siebers et al., 2016). Consequently, $\delta^{18}O$ and $\delta^{2}H$ values can be used as a continuous indicator of water source and evaporation, with higher values indicating progressive disconnection and evaporation from source. In Coondiner, $\delta^{18}O$ values of CND1 (-6.49 ‰) reflected high alluvial water connectivity and those of CND3 (-1.85 ‰) and CND4 (13.1 ‰) showed progressively further evaporation from source. In Ben's Oasis, BO4 (-7.14 ‰) likely had higher alluvial water connectivity than BO3 (-3.05 ‰) (Figure A.1).

*Field methods*

In pools CND3 and BO3 (the two main study pools), water samples for $\delta^{13}C_{DIC}$, $\delta^{18}O$ and $\delta^{2}H$, dissolved organic matter (DOM), and inorganic nutrient (N, P) analysis were taken every 2 hrs over 26-28 hours. Two 40 mL water samples were collected at 5 cm below the surface, filtered immediately through 0.2 µm sterile PES syringe filters, and stored without headspace in airtight, sterile glass vials at 4°C in the dark until analysis. In all pools, dissolved oxygen (DO) and temperature were recorded in surface water (20 cm depth) at 15 minute intervals over 48-50 hrs using a TPS WP-82Y DO-temperature meter and autologger

in combination with an EDYSI DO sensor (Yellow Springs, OH, USA). Sensors were placed at the approximate thalweg of each pool. Despite the high range of air temperature, preliminary depth profiles indicated no temperature stratification in pools. However, it was logistically impossible to obtain temperature profiles across diel cycles. Cloud cover was absent in the mornings, but increased to low amounts (< 30 %) in the afternoons during each measurement period.

For all pools, electrical conductivity (EC) was measured using a YSI 85 handheld probe (Yellow Springs, OH, USA) and pH using a handheld ecoTestr pH 2 probe (Vernon Hills, IL, USA) before water samples were taken. A water sample was collected as described for diel sampling (above) for analysis of $\delta^{18}O$, $\delta^{2}H$, nutrients (N, P) and DOM. At Coondiner, photosynthetically active radiation (PAR), wind speed and direction, air temperature, relative humidity, and cumulative rainfall were measured at 15 min intervals using a HOBO weather station situated ca. 200-m north of CND1; data extended continuously back from the sampling period to October 2010.

All pools were mapped for length, width, depth, aspect, cover of terrestrial and aquatic vegetation, and distance to and height of adjoining gorge walls in the field (see Table 1). Maps of each pool at the time of sampling were created from pool morphology maps cross-referenced with GPS points taken in the field. All maps were converted to georeferenced shapefiles and the area of pools ($m^2$) and area of aquatic vegetation within pools ($m^2$) were calculated in QGIS ver. 2.16.3 (Quantum GIS Development Team, http://qgis.osgeo.org). We calculated aquatic vegetation cover (%) in each pool as the percentage contribution of aquatic vegetation area within the total pool area.

*Analytical methods*

Water samples (1 mL) for $\delta^{13}C_{DIC}$ were acidified under $He_2$ atmosphere with orthophosphoric acid (0.1 mL of 100 % $H_3PO_4$), and the produced $CO_{2(gas)}$ was analysed using a GasBench II coupled with a Thermo-Fisher Delta XL Mass Spectrometer (Bremen, Germany). $\delta^{13}C_{DIC}$ values are given in per mil (‰, VPDB) according to delta notation, following three-point normalization based on international standards provided by IAEA (L-SVEC, NBS19, and NBS18) used in order to reduce raw values to the international scale (Skrzypek, 2013). Values of international standards for carbon ($\delta^{13}C$) are from Coplen et al. (2006). The analytical error of $\delta^{13}C$ analysis is <0.10‰.

Stable isotope composition ($\delta^{18}O$, $\delta^{2}H$) of each water sample was analyzed using a Picarro L1102-i Isotopic Liquid Water Analyser (Santa Clara, CA, USA). $\delta^{18}O$ and $\delta^{2}H$ values are reported in per mil (‰) after normalization to VSMOW2 scale (Vienna Standard Mean Ocean Water), following a three-point normalization using three laboratory standards each replicated twice (Coplen, 1994). All laboratory standards were calibrated against international reference materials for the VSMOW2/SLAP (Standard Light Antarctic Precipitation, relative to VSMOW2) scale provided by the International Atomic Energy Agency (Coplen, 1995). Analytical precision was 1.0 ‰ for $\delta^{2}H$ and 0.1 ‰ for $\delta^{18}O$.

Soluble reactive phosphorus (SRP; free $PO_4$-P) was measured using the ascorbic acid method (Murphy and Riley, 1962) with a detection limit of 2.5 µg P $L^{-1}$. Dissolved inorganic nitrogen (DIN; $NH_4$-N and $NO_3$-N) was determined by spectrophotometric colorimetric detection method on a Technicon auto-analyzer (Tarrytown, NY, USA) with a detection limit of 8 µg N $L^{-1}$. DOM was analyzed by excitation-emission fluorescence spectroscopy on a Varian Cary Eclipse fluorometer (Mulgrave, VIC, Australia). The fluorescence index (FI) of dissolved organic matter (DOM) was calculated as the ratio of fluorescence intensity at emission wavelengths of 450 and 500 nm, at an excitation wavelength of 370 nm as an indicator of the

possible source of DOM (McKnight et al., 2001). Excitation and Emission slit widths were 5 nm and photomultiplier tube voltage was set at 725 v. Samples were corrected for inner filter effects, by dilution with Milli-Q water, when optical density was > 0.05 at 254 nm within a 1 cm quartz cuvette (Green and Blough, 1994).

*Modelling of ecosystem metabolism*

We used the Bayesian Single-station Estimation (BASE) model (v 2.3) of Grace et al. (2015) to estimate gross primary productivity (GPP; mg $O_2$ $L^{-1}$ $d^{-1}$) and ecosystem respiration (ER; mg $O_2$ $L^{-1}$ $d^{-1}$) for each pool. We used a five-parameter BASE model that simultaneously estimates the temperature dependence of respiration (Θ) and light saturation of photosynthesis (*p*) along with re-aearation flux (*k*), GPP, and ER (Grace et al., 2015). The night-time regression method for estimating *k* across pools (Hornberger and Kelly, 1975) had variable explanatory power (generalised linear model $R^2$ = 0 to 0.82). Because pools were lentic environments at the time of sampling, we created estimates of *k* across pools following Staehr et al. (2010). At each 15-min time step of the DO measurements, we calculated *k* (m $h^{-1}$) using the equations of Cole and Caraco (1998) and Jähne et al. (1987) with wind speed data from the local weather station (Smith, 1985) and a Schmidt coefficient derived from water temperature (Wanninkhof, 1992). The *k* (m $h^{-1}$) values were then multiplied by 24 to give units of m $d^{-1}$. Mean and standard deviation for daily *k* (m $d^{-1}$) were then calculated across all pools. Mean estimated *k* was 0.3 m $d^{-1}$ (SD = 0.03 m $d^{-1}$), and these values were used as informative priors for *k* in the BASE models. DO data were smoothed with a fast Fourier transformation before modelling to reduce variation in signal noise, and thus variation in the slope of DO change with time (as in e.g. Oliver and Merrick, 2006). PAR was smoothed by a moving average across 5 time periods before modelling. Atmospheric pressure was estimated from stream altitude (Grace and Imberger, 2006). Salinity was estimated at zero as EC

measures were <1000 µS $cm^{-1}$ (WEF & APHA, 2005). The BASE package was run in R v 3.4.2 (R Core Team 2012) using 100,000 iterations with the first 50,000 discarded.

For comparison with other datasets and to adjust for differences in pool volume, GPP and ER measurements were converted to area (g $O_2$ $m^{-2}$ $d^{-1}$) by multiplying with average depth of each pool (Grace and Imberger, 2006). GPP and ER were then further converted to units of carbon (g C $m^{-2}$ $d^{-1}$) using the ratio of atomic mass of C to molecular mass of $O_2$, a photosynthetic quotient (number of moles of $O_2$ released per mole of $CO_2$ incorporated) of 1.2, and respiratory quotient (number of moles of $CO_2$ released per mole of $O_2$ consumed) of 0.85 (Bott 2006).

*Data analysis*

Measured variables ($\delta^{13}C_{DIC}$, DO, temperature, $\delta^{18}O$, $\delta^{2}H$, water chemistry) were predicted by time (hours since the start of sampling) using generalised additive models (GAMs) to assess diel cycles occurring in CND3 and BO3. DO concentrations (mg $L^{-1}$) were first converted to % saturation (Grace and Imberger, 2006) to reduce possible signal noise due to temperature-solubility effects. Diel changes were indicated when time was a significant ($p < 0.05$) predictor.

We used Bayes Factors (BFs) and generalised linear models (GLMs) to identify possible drivers of $\delta^{13}C_{DIC}$ over the diel cycle in CND3 and BO3. $\delta^{2}H$ values were not included as a predictor as they largely covary with $\delta^{18}O$, but can also induce noise due to variation in local humidity conditions (Gat, 1996). Instantaneous rates of GPP and ER were further not included, as in metabolism models they essentially covary with PAR and temperature, respectively (Grace et al., 2015, Appling et al., 2018). We thus consider PAR and

temperature as proxies for these rates. First, we calculated BFs for linear regressions (Rouder and Morey, 2012), predicting $\delta^{13}C_{DIC}$ from corresponding DO, $\delta^{18}O$, PAR, DIN, and temperature measures (Table A.1) and their interaction terms. Predictors for the model with the highest BF (i.e., the model with the greatest multiplicative increase in explanatory power relative to an intercept-only model) were then used to create GLMs. All GLMs were modeled using a temporal autocorrelation term based on sampling time. If any predictor term (not including intercept) was non-significant ($p > 0.05$) in the GLM, it was discarded and the model with the next best BF was used. Second, we assessed whether changes in $\delta^{13}C_{DIC}$ between time periods were of similar magnitude to changes in other measured parameters. The change in $\delta^{13}C_{DIC}$ over time ($\Delta^{13}C_{t2\text{-}t1}$, ‰ hour$^{-1}$) as well as DO, $\delta^{18}O$, PAR, DIN, and temperature was calculated at each 2-hour time step. Then, BFs and GLMs were used, as above, to identify the best predictors of $\Delta^{13}C_{t2\text{-}t1}$.

We calculated BFs (relative to an intercept-only model) for each possible multiple linear regression predicting GPP and ER, including pool hydrology, size, and water chemistry measurements. Pool area data were not normally distributed (Shapiro-Wilk test, $p = 0.003$), thus values were natural log-transformed before analysis. All other predictors were normally distributed. Areal rates (g $O_2$ m$^{-2}$ d$^{-1}$) were used for GPP and ER models. Predictors for the model with the highest BF were used to create GLMs. Due to the low sample size of metabolic measures (5), we present the model with the best BF here regardless of GLM significance. Mean GPP and ER values from the BASE analysis were used. We used positive rather than negative signs on values of ER for conceptual clarity (i.e., if a predictor has a positive correlation with ER, then ER rates increase with increasing values of the predictor). BASE estimates are technically derived from posterior distributions rather than true sample means, but standard deviations of BASE estimates were small (0.04 to 0.87, Table 2). This

infers that GLM results provided an accurate estimation of correlations with true population GPP and ER means. All statistical analyses were conducted in R v3.41 (R Core Team 2017). GAMs and GLMs were done using the R package mgcv (v 1.8) and Bayes factors were calculated using the package BayesFactor (v. 0.9.10.2).

## Results

Pools differed substantially in primary producers at the time of sampling. At Coondiner, CND1 was dominated by charophytes (*Chara* spp.), emergent (*Typha orientalis*, *Schoenoplectus subulatis*) and floating (*Potamogeton tricarinatus*) aquatic macrophytes, and attached filamentous algae (*Spyrogyra* spp.), occurring along a 1-3 m wide margin around the pool. CND3 was shallow (average 0.14 m deep) with charophytes and filamentous algae restricted to narrow (<1 m) patches along the pool margin, whereas water in CND4 was opaque from green algae. Lastly, there was terrestrial leaf litter (predominantly *Eucalyptus* and *Melaleuca* spp.) on the bed of all pools, except CND4. At Ben's Oasis, water of pool BO3 was tannin rich, with aquatic macrophytes confined to small (<1 $m^2$), sporadic patches along shallow margins. The pool was deep, but dense riparian woodland suggested there was likely to be terrestrial organic matter on the bottom. Water of BO4 was tannin rich, shallow (average 0.4 m deep), and aquatic macrophytes and terrestrial leaf litter abundant. Both pools had dense riparian woodlands.

### *Diel biogeochemical cycles*

$\delta^{13}C_{DIC}$ showed regular diel patterns at both CND3 ($p < 0.001$) and BO3 ($p < 0.001$), with increasing values during the day balanced by decreasing values during the night (Fig. 2a, b). Average $\delta^{13}C_{DIC}$ values were -10.29 ‰ in CND3 and -12.53 ‰ in BO3. Diel amplitude in

$\delta^{13}C_{DIC}$ values differed slightly between the two pools (CND3 = 0.91 ‰, BO3 = 0.64 ‰). Water temperatures also exhibited consistent diel variation in CND3 ($p < 0.001$) and BO3 ($p < 0.001$), with warmest temperatures (25-27°C) at 16:00 decreasing to coolest (20-23°C) just after dawn (Fig. 2c, d). Dissolved oxygen (DO) also exhibited diel variation at CND3 ($p < 0.001$) and BO3 ($p < 0.001$). However, both the time of maxima (CND = 14:40, BO3 = 18:55) and diel amplitude (CND = 28 %, BO3 = 8.1 %) in DO % saturation differed between pools (Fig. 2e, f).

Water $\delta^{18}O$ values exhibited no consistent diel trends at CND3 ($p = 0.19$) or BO3 ($p = 0.35$). Water $\delta^{2}H$ values also exhibited no consistent diel trends at BO3 ($p = 0.98$), but $\delta^{2}H$ values decreased steadily over time at CND3 ($p = 0.024$, Fig. A.2). Dissolved inorganic P (SRP) was below detection limits (<2.5 µg $L^{-1}$) in all samples. Fluorescence Index (FI) values ($p = 0.9$, 0.8, CND3 and BO3, respectively), $NH_4$ concentrations ($p = 0.19$, 0.15, respectively), and $NO_3$ concentrations ($p = 0.08$, 0.23, respectively) exhibited no diel patterns in either pool.

*Drivers of $\delta^{13}C_{DIC}$*

The best predictor of $\delta^{13}C_{DIC}$ values at CND3 was water temperature (BF = 12618.8). The temperature model had ca 5.1 times more explanatory power than the next best model, temperature + PAR (BF = 2460.7), and ca. 6.1 times more explanatory power than the best model containing DO as a predictor (temperature + DO, BF = 2054.5). $\delta^{13}C_{DIC}$ values at CND3 were higher when water temperature was higher (standardised a = 0.94 ± 0.01, Fig. 3a). The best predictor of change in $\delta^{13}C_{DIC}$ over time ($\Delta^{13}C_{t2\text{-}t1}$, ‰) at CND3 was also temperature (BF = 7.23). An increase or decrease in temperature was linearly correlated with a concurrent increase or decrease in $\delta^{13}C_{DIC}$ at CND3 (standardised a = 0.71 ± 0.21, intercept $p = 0.93$, Fig. 3b).

The best predictor of $\delta^{13}C_{DIC}$ values at BO3 was temperature + PAR (BF = 248212.7). The next best model, temperature + DO + PAR, had ca. 7.4 times less explanatory power (BF = 33404.9), and DO was not a significant predictor in the corresponding GLM (p = 0.6). $\delta^{13}C_{DIC}$ values at BO3 were higher when water temperature was higher (standardised a = 0.94 ± 0.06) and when PAR was higher (standardised a = 0.29 ± 0.06, Fig. 4a). The best predictors of $\Delta^{13}C_{t2\text{-}t1}$ at BO3 were also changes in temperature and PAR (BF = 116.8). $\delta^{13}C_{DIC}$ increased concurrently with increases in temperature (standardised a = 0.83 ± 0.14) and PAR (standardised a = 0.42 ± 0.14; intercept p = 0.86, Fig. 4b).

*Ecosystem metabolism*

The diel amplitude in DO values differed across the larger set of pools, ranging from 0 to 8 mg $L^{-1}$ at Coondiner to 0.1 to 1.4 mg $L^{-1}$ in Ben's Oasis (Table 2). Gross primary production (GPP; 1.25 to 10.75 mg $O_2$ $L^{-1}$ $d^{-1}$) and ecosystem respiration (ER; 3.03 to 11.95 mg $O_2$ $L^{-1}$ $d^{-1}$) estimates also varied across pools, although all pools were heterotrophic (Table 2). The best predictors of GPP (BF = 3.59) were pool area, vegetation cover, and FI values. GPP was highest in larger pools with higher aquatic vegetation cover as well as higher FI values (Fig. 5). The best predictors of ER (BF = 1.56) were GPP, vegetation cover, and FI values. ER was highest in more productive pools, but with lower aquatic vegetation cover and FI values (Fig. 5). GPP:ER ratios were best predicted (BF = 1.32) by aquatic vegetation area, vegetation cover, and FI values. GPP:ER ratios were thus highest in pools with higher aquatic vegetation area and cover, as well as higher FI values (Fig. 5).

## Discussion

*Drivers of $\delta^{13}C_{DIC}$ cycles*

The $\delta^{13}C_{DIC}$ values measured here, ca. -10 to -11 ‰ at Coondiner and -12 to -13 ‰ at Ben's Oasis, were similar to values of relatively large lakes with neutral pH and low primary production (Bade et al., 2004) and mid-size streams with significant groundwater contributions (Finlay, 2003). The different baselines for $\delta^{13}C_{DIC}$ between catchments likely reflect differences in underlying groundwater geochemistry (Dogramaci et al., 2015), as pools in both streams were likely connected to shallow alluvial throughflow earlier in the year (Siebers et al. 2016). For Coondiner, values were relatively enriched compared to alluvial water ($\delta^{13}C_{DIC}$ was -13.7 and -17.7 ‰ in the alluvial bore at Coondiner Creek gorge outlet; Skrzypek, unpubl. data). Higher average $\delta^{13}C_{DIC}$ values might thus reflect increased photosynthetic fractionation of DIC (Finlay, 2003) once CND3 was disconnected from alluvial throughflow.

Diel patterns of $\delta^{13}C_{DIC}$ were highly consistent and much less variable across pools than those of dissolved oxygen. These results contrast with studies of eutrophic, autotrophic, and perennial streams that typically show corresponding variation in diel ranges of both $\delta^{13}C_{DIC}$ and DO (Parker et al. 2005, 2010; Tobias and Böhlke, 2011). Instead, we observed strong correlations between $\delta^{13}C_{DIC}$ and water temperature. ER rates typically covary with respiration rates (Grace et al., 2015, Appling et al., 2018). However, increasing ER rates should decrease $\delta^{13}C_{DIC}$ values through production of $CO_2$ reflecting relatively depleted organic matter sources (Finlay, 2003). Instead, we observed increases in $\delta^{13}C_{DIC}$ with temperature. Further, the magnitude of change in $\delta^{13}C_{DIC}$ with temperature was consistent at both CND3 ($a = 0.163 \pm 0.05$) and BO3 ($a = 0.162 \pm 0.02$) despite differences in daily ER estimates. It is thus unlikely that changes in ER rates alone would drive changes in $\delta^{13}C_{DIC}$.

Conversely, GPP rates covary with PAR (Mulholland et al., 2001, Grace et al., 2015, Appling et al., 2018) but can also increase with temperature (Rasmussen et al., 2011). It is thus

possible that the balance between ER-driven decreases in $\delta^{13}C_{DIC}$ were balanced by similar temperature-driven increases in photosynthetic fractionation rates across both pools (Tobias et al., 2007), despite the overall differences in GPP and ER rates. While the effect size was smaller than for temperature, we did observe corresponding increases in $\delta^{13}C_{DIC}$ and PAR at BO3. However, we also estimated differences in GPP:ER ratios between BO3 and CND3. Further, CND3 had benthic charophytes, which are noteworthy among aquatic macrophytes for their ability to photosynthetically assimilate soluble bicarbonates (Kufel and Kufel, 2002). $\delta^{13}C_{DIC}$ typically increases above photosynthesising charophyte stands (Pronin et al., 2016) due to significant fractionation during $HCO_3^-$ uptake and associated $CaCO_3$ precipitation (McConnaughey, 1998). During the day, respiration-derived $CO_2$ might also be largely contained within charophyte stands due to highly localized stratification effects (Andersen et al., 2019). We would thus expect to see higher rates of change in water column $\delta^{13}C_{DIC}$ within CND3, rather than similar amplitudes to BO3.

Multiple, recent studies have indicated that small streams (see Hotchkiss et al., 2015 and references therein) and ponds (Holgerson and Raymond, 2016) have high rates of $CO_2$ efflux due to small surface areas and high connectivity with the terrestrial landscape. As all of the pools were heterotrophic and lentic environments, $CO_2$ concentrations were likely above saturation (Sobek et al., 2005, Holgerson and Raymond 2016). Further measurements at Coondiner Creek also indicate that $pCO_2$ is greater than in the atmosphere (J. Iles, pers. comm. unpubl. data). The solubility of $CO_2$ decreases with temperature, and kinetic fractionation of $\delta^{13}C_{DIC}$ might thus increase with temperature due to increases in outgassing rates. In addition, as chemical equilibrium between DIC species does not occur in open systems, equilibrium fractionation amplifies changes in $\delta^{13}C_{DIC}$ when outgassing occurs (Doctor et al., 2008). The temperature-dependent range of $\delta^{13}C_{DIC}$ equilibrium fractionation

(between $HCO_3^-{}_{(aq)}$ and $CO_{2(gas)}$) due to outgassing corresponds to 0.88 ‰ in CND3 and 0.72 ‰ in BO3 (Marlier and O'Leary, 1984), close to the diurnal amplitude of $\delta^{13}C_{DIC}$ values seen here (CND3 = 0.90 ‰, BO3 = 0.64 ‰). Further, $CO_2$ outgassing rates in pools are likely limited by reaeration rates even when $pCO_2$ is high (Gómez-Gener et al., 2015), and estimated rearation rates were similar between CND3 and BO3. We suggest that, given the role of small freshwater environments as "$CO_2$ chimneys" (Cole et al., 2007, Battin et al., 2008, Hotchkiss et al., 2015), the role of outgassing in drving $\delta^{13}C_{DIC}$ cycles within pools or small ponds would thus be a productive area of future study.

There was little evidence for diel changes in $\delta^{18}O$ or $\delta^{2}H$ at BO3, and $\delta^{18}O$ values suggest CND3 was disconnected from alluvial throughflow. Thus, is appears unlikely that diurnal variation in alluvial groundwater throughflow affected diel cycles of $\delta^{13}C_{DIC}$ at either pool. However, development of anoxic conditions during the night could also lead to diurnal variation in methanogenesis or methane oxidation. The fractionation effect of both processes is large, but the net effect should be increased $\delta^{13}C_{DIC}$ values (Campeau et al., 2018). Although the diel variation in $\delta^{13}C_{DIC}$ was small here, even slight increases in methane-associated processes might thus buffer respiration-driven night-time decreases in $\delta^{13}C_{DIC}$. Overall, multiple processes might thus be acting at different rates to produce the same $\delta^{13}C_{DIC}$ values and buffer diurnal cycles (Campeau et al., 2017), and we would require accurate measurements of each to fully partition $\delta^{13}C_{DIC}$ variation ("equifinality", as with ecosystem metabolism measurements; sensu Appling et al., 2018). Ultimately, we would thus require more detailed measurements of the concentration, and stable isotope composition, of the different DIC species to fully conclude which processes drive diurnal variation in $\delta^{13}C_{DIC}$ here.

*Relationships between ecosystem metabolism and hydrology*

All of the pools measured here were heterotrophic, despite differences in aquatic vegetation composition and cover. Macrophyte-rich, DOC-poor lentic systems can be autotrophic, but usually when nutrients are not limiting (Duarte and Prairie, 2005). Both phytoplankton and charophyte metabolism is largely limited by oligotrophic conditions in Coondiner Creek (Iles, 2019). Shallow pools or ponds are also unlikely to be organic carbon-limited due to high perimeter-to-edge ratios and extensive contact between the water column and sediment (Holgerson, 2015). Further, in the absence of surface flow the downstream export of both allochthonous and autochthonous organic matter largely ceases (Fisher et al., 1998b, Acuña et al., 2004). Respiration of organic matter should thus occur where it originated as opposed to various points along downstream flowpaths (Battin et al., 2008, Larned et al., 2010). Even small inputs of terrestrial organic matter are thus likely to lead to consistently heterotrophic conditions across these pools, regardless of GPP rates.

When converted to terms of carbon produced, rates of GPP (0.11 to 0.55 g C $m^{-2}$ $d^{-1}$) and ER (0.16 to 0.84 g C $m^{-2}$ $d^{-1}$) measured here were at the lower ranges of ecosystem metabolism for dryland rivers (Bunn et al., 2006a) but comparable to those of lowland river waterholes in central Australia (Fellows et al., 2007). However, the latter systems tend to be turbid and characterized by high benthic algal production in narrow photic zones (Bunn et al., 2003). Areal rates of ER also were low (0.5 to 2.6 g $O_2$ $m^{-2}$ $d^{-1}$) compared to other dryland streams with high retention of terrestrial organic matter (Acuña et al., 2004). The macrophyte-dominated Coondiner Creek is thus more analogous to the low-nutrient, alluvial groundwater-maintained Daly River in sub-tropical northern Australia (Webster et al., 2005).

Under low nutrient concentrations, primary production can be limited by light availability (Karlsson et al., 2009). Dryland streams often have relatively open riparian vegetation unlikely to cause significant light limitation (e.g. Bunn et al. 1999). However, preliminary

data on light penetration at Coondiner shows attenuation coefficients can be as high as 0.97 within the first 0.5-0.6 m of water (J. Kelley, pers. comm. unpubl. data). High concentrations of humic DOM (Siebers et al. 2016) may thus limit light availability to benthic primary producers (Karlsson et al., 2009). Further, if algal growth rates are restricted by oligotrophic conditions, photosynthesis can result in GPP fuelling the production and release of labile DOM (Townsend et al., 2011). Dryland pools typically have higher proportions of autochthonous DOM after cessation of flow (Fellman et al., 2011; Vazquez et al., 2011). Further, Australian riparian trees are largely sclerophyllous and thus highly recalcitrant (Francis and Sheldon, 2002). Light might thus also limit ER rates overall, if microbial communities preferentially respire algal DOM (Mulholland et al. 2001).

Contrary to our predictions, $\delta^{18}O$ and $\delta^{2}H$ values (reflecting the overall hydrological regime, and thus likely an important driver of both GPP and ER) were not among the best predictors of ecosystem metabolism. Instead, pool size and aquatic vegetation cover were highly correlated with GPP, ER, and GPP:ER ratios. The main influence of alluvial groundwater inputs on ecosystem metabolism is thus likely in alleviating evaporative contraction (Siebers et al. 2016), which should reduce disturbance of aquatic primary producers and increase GPP (Stanley et al. 1997). However, cessation of surface flow and subsequent loss of upstream subsidies (e.g. Wiegner et al., 2005) might increase internal cycling of nutrients and organic matter within microbial communities (Mulholland et al., 1995). This internal recycling can increase regardless of production rates, particularly under oligotrophic conditions (Mulholland et al., 1991, Scott et al., 2008). The charophyte communities abundant in Coondiner Creek after cessation of flow may further act as nutrient sinks and sites of increased microbial metabolism (Kufel and Kufel, 2002). Nutrient inputs from alluvial groundwater might thus still support higher autotrophic biomass or productivity, but not be

reflected in water column chemistry.

Further, Coondiner Creek is largely dominated by benthic charophytes and floating (*Potamogeton* spp.) and emergent (*Typha* spp., *Schoenoplectus* spp.) aquatic vegetation. As with DIC dynamics (see above), charophytes can form anoxic zones within stands (Anderson et al., 2019) but also oxygenate sediments through rhizome leakage (Kufel and Kufel, 2002). Conversely, macrophytes with floating or emergent leaves largely exchange oxygen and $CO_2$ directly with the atmosphere (Pinardi et al., 2011, Attermeyer et al., 2016). Deoxygenated water uptake by riparian vegetation can also significantly affect in-stream DO measurements (Dodds et al. 2017). During drying, recently emerged sediments might also support substantial respiration rates (Gómez-Gener et al. 2016), possibly affecting DO dynamics in neighbouring littoral areas. If dissolved oxygen is substantially affected by "ex-situ" exchange or processes, then water column DO measurements might significantly underestimate ecosystem metabolism.

*Conclusions*

We observed similar diurnal amplitudes of $\delta^{13}C_{DIC}$ in ephemeral stream pools, despite pronounced differences in DO cycles. However, these patterns may not reflect differences between rates of ecosystem metabolism and DIC cycling. Oxygen cycling was likely not confined to fully aquatic processes, or might have been rapidly cycled within ecosystem compartments (e.g. biofilms, charophyte stands) without exchange in the bulk water column. Relatively low Bayes Factor values (< 3.0, see e.g. Dienes, 2014) and low sample size (5) also largely restrict our conclusions as to the drivers of GPP and ER. Further, estimates of ecosystem metabolism are notably sensitive to errors in reaeration estimates and other model parameters (McCutchan et al., 1998, Demars et al., 2015, Appling et al. 2018). Similarly,

cycling of various DIC species might have been highly compartmentalized within the pools we sampled. As freshwater environments dry and contract, drivers of ecological processes become increasingly more localized (Fisher et al., 1998b, Larned et al., 2010, Humphries et al., 2014). The physical and chemical characteristics of dryland stream pools can thus become highly spatially and temporally heterogeneous (e.g. Vazquez et al. 2011). We suggest that, in pools of other dryland streams, metabolic cycling of oxygen and $CO_2$ might thus be highly compartmentalized within fine-scale biogeochemical hotspots across both space and time.

## References


Acuña, V., A. Giorgi, I. Muñoz, U. Uehlinger, and S. Sabater S. 2004. Flow extremes and benthic organic matter shape the metabolism of a headwater mediterranean stream. Freshwater Biol. 49: 960-971.

Andersen, M. R., T. Kragh, K. T. Martinsen, E. Kristensen, and K. Sand-Jensen. 2019. The carbon pump supports high primary production in a shallow lake. Aquat. Sci. 81: 24.

Appling, A. P., R. O. Hall Jr, C. B. Yackulic, and M. Arroita. 2018. Overcoming equifinality: Leveraging long time series for stream metabolism estimation. J. Geophys. Res.-Biogeo. 123: 624-645.

Attermeyer, K., S. Flury, R. Jayakumar, P. Fiener, K. Steger, V. Arya, ... and K. Premke. 2016. Invasive floating macrophytes reduce greenhouse gas emissions from a small tropical lake. Sci. Rep. 6: 20424.

Bade, D. L., S. R. Carpenter, J. J. Cole, P. C. Hanson, and R. H. Hesslein. 2004. Controls of $\delta^{13}$C-DIC in lakes: Geochemistry, lake metabolism, and morphometry. Limnol. Oceanogr. 49: 1160-1172.

Bastviken, D., J. J. Cole, M. L. Pace, and M. C. Van de Bogert. 2008. Fates of methane from different lake habitats: Connecting whole- lake budgets and $CH_4$ emissions. J.

Geophys. Res.-Biogeo. 113: G02024.

Battin, T.J., Kaplan, L.A., Findlay, S., Hopkinson, C.S., Marti, E., Packman, A.I., Newbold, J.D. and Sabater, F., 2008. Biophysical controls on organic carbon fluxes in fluvial networks. Nat. Geosci. 1: 95.

Bott, T. L. 2006. Primary productivity and community respiration, p. 533-556. In: F. R. Hauer and G. A. Lamberti [eds], Methods in Stream Ecology (2nd ed.). Academic Press, San Diego.

Bunn, S. E., P. M. Davies, and T. D. Mosisch. 1999. Ecosystem measures of river health and their response to riparian and catchment degradation. Freshwater Biol. 41: 333-345.

Bunn, S. E., P. M. Davies, and M. Winning. 2003. Sources of organic carbon supporting the food web of an arid zone floodplain river. Freshwater Biol. 48: 619-635.

Bunn, S. E., S. R. Balcombe, P. M. Davies, C. S. Fellows, and F. J. Mckenzie-Smith. 2006a. Aquatic productivity and food webs of desert river ecosystems, p. 76-99. In: R.T. Kingsford [ed], Ecology of Desert Rivers. Cambridge University Press.

Bunn, S. E., M. C. Thoms, S. K. Hamilton, and S. J. Capon. 2006b. Flow variability in dryland rivers: boom, bust and the bits in between. River. Res. Appl. 22: 179-186.

Campeau, A., M. B. Wallin, R. Giesler, S. Löfgren, C. M. Mörth, S. Schiff, ... and K. Bishop. 2017. Multiple sources and sinks of dissolved inorganic carbon across Swedish streams, refocusing the lens of stable C isotopes. Sci. Rep. 7: 9158.

Campeau, A., K. Bishop, M. B. Nilsson, L. Klemedtsson, H. Laudon, F. I. Leith, ... and M. B. Wallin. 2018. Stable carbon isotopes reveal soil- stream DIC linkages in contrasting headwater catchments. J. Geophys. Res.–Biogeo. 123: 149-167.

Capone, T. A., and J. A. Kushlan. 1991. Fish community structure in dry-season stream pools. Ecology 72: 983-992.

Casas-Ruiz, J. P., J. Tittel, D. von Schiller, N. Catalán, B. Obrador, L. Gómez-Gener, E.

Zwirnmann, S. Sabater, and R. Marcé. 2016. Drought-induced discontinuities in the source and degradation of dissolved organic matter in a Mediterranean river. Biogeochemistry 121: 125-139.

Cole, J. J., and N. F. Caraco. 1998. Atmospheric exchange of carbon dioxide in a low-wind oligotrophic lake measured by the addition of SF6. Limnol. Oceanogr. 43: 647-656.

Cole, J. J., Y. T. Prairie, N. F. Caraco, W. H. McDowell, L. J. Tranvik, R. G. Striegl, C. M. Duarte, P. Kortelainen, and others. 2007. Plumbing the global carbon cycle: integrating inland waters into the terrestrial carbon budget. Ecosystems 10: 172-185.

Coplen, T. B. 1994. Reporting of stable hydrogen, carbon, and oxygen isotopic abundances. Pure Appl. Chem. 66: 273-276.

Coplen, T. B. 1995. Discontinuance of SMOW and PDB. Nature 375: 285-285.

Coplen, T. B., W. A. Brand, M. Gehre, M. Gröning, H. a. J. Meijer, B. Toman, and R. M. Verkouteren. 2006. New guidelines for $\delta^{13}C$ measurements. Anal. Chem. 78: 2439-2441.

Dahm, C. N., M. A. Baker, D. I. Moore, and J. R. Thibault. 2003. Coupled biogeochemical and hydrological responses of streams and rivers to drought. Freshwater Biol. 48: 1219-1231.

Demars, B. O. L., J. Thompson, and J. R. Manson. 2015. Stream metabolism and the open diel oxygen method: Principles, practice, and perspectives. Limnol. Oceanogr. Methods 13: 356–374.

Dienes, Z. 2014. Using Bayes to get the most out of non-significant results. Front. Psychol. 5: 781.

Doctor, D. H., C. Kendall, S. D. Sebestyen, J. B. Shanley, N. Ohte, and E. W. Boyer. 2008. Carbon isotope fractionation of dissolved inorganic carbon (DIC) due to outgassing of carbon dioxide from a headwater stream. Hydrol. Process. 22: 2410-2423.

Dodds, W. K., F. Tromboni, W. Aparecido Saltarelli, and D. G. Fernandes Cunha. 2017. The root of the problem: Direct influence of riparian vegetation on estimation of stream ecosystem metabolic rates. Limnol. Oceanogr. 2: 9-17.

Dogramaci, S., G. Skrzypek, W. Dodson, and P. F. Grierson. 2012. Stable isotope and hydrochemical evolution of groundwater in the semi-arid Hamersley Basin of subtropical northwest Australia. J. Hydrol. 475: 281-293.

Dogramaci, S., G. Firmani, P. Hedley, G. Skrzypek, and P. F. Grierson. 2015. Evaluating recharge to an ephemeral dryland stream using a hydraulic model and water, chloride and isotope mass balance. J. Hydrol. 521: 520-532.

Drysdale, R., S. Lucas, and K. Carthew. 2003. The influence of diurnal temperatures on the hydrochemistry of a tufa-depositing stream. Hydrol. Process. 17: 3421-3441.

Duarte, C. M., and Y. T. Prairie. 2005. Prevalence of heterotrophy and atmospheric $CO_2$ emissions from aquatic ecosystems. Ecosystems 8: 862-870.

Farquhar, G. D., J. R. Ehleringer, and K. T. Hubick. 1989. Carbon isotope discrimination and photosynthesis. Annu. Rev. Plant Phys. 40: 503-537.

Fellman, J. B., S. Dogramaci, G. Skrzypek, W. Dodson, and P. F. Grierson. 2011. Hydrologic control of dissolved organic matter biogeochemistry in pools of a subtropical dryland river. Water Resour. Res. 47: W06501, doi: 10.1029/2010WR010275

Fellman, J. B., R. G. M. Spencer, P. A. Raymond, N. E. Pettit, G. Skrzypek, P. J. Hernes, and P. F. Grierson. 2014. Dissolved organic carbon biolability decreases along with its modernization in fluvial networks in an ancient landscape. Ecology 95: 2622-2632.

Fellows, C. S., M. L. Wos, P. C. Pollard, and S. E. Bunn. 2007. Ecosystem metabolism in a dryland river waterhole. Mar. Freshw. Res. 58: 250-262.

Fellows, C. S., S. E. Bunn, F. Sheldon, and N. J. Beard. 2009. Benthic metabolism in two turbid dryland rivers. Freshwater Biol. 54: 236-253.

Finlay, J. 2003. Controls of streamwater dissolved inorganic carbon dynamics in a forested watershed. Biogeochemistry 62: 231-252.

Fisher, S. G., N. B. Grimm, E. Martí, and R. Gómez. 1998a. Hierarchy, spatial configuration, and nutrient cycling in a desert stream. Aust. J. Ecol. 23: 41-52.

Fisher, S. G., N. B. Grimm, E. Martí, R. M. Holmes, and J. J. B. Jones. 1998b. Material spiraling in stream corridors: a telescoping ecosystem model. Ecosystems 1: 19-34.

Francis, C., and F. Sheldon. 2002. River Red Gum (Eucalyptus camaldulensis Dehnh.) organic matter as a carbon source in the lower Darling River, Australia. Hydrobiologia 481: 113-124.

Gat, J. R. 1996. Oxygen and hydrogen isotopes in the hydrologic cycle. Annu. Rev. Earth Planet. Sci. 24: 225-262.

Gómez-Gener, L., B. Obrador, D. von Schiller, R. Marcé, J. P. Casas-Ruiz, L. Proia, ... and M. Koschorreck. 2015. Hot spots for carbon emissions from Mediterranean fluvial networks during summer drought. Biogeochemistry 125: 409-426.

Gómez-Gener, L., B. Obrador, R. Marcé, V. Acuña, N. Catalán, J. P. Casas-Ruiz, S. Sabater, I. Muñoz, and D. von Schiller, 2016. When water vanishes: magnitude and regulation of carbon dioxide emissions from dry temporary streams. Ecosystems 19: 710-723.

Grace M, and S. Imberger. 2006. Stream metabolism: performing and interpreting measurements. Murray Darling Basin Commission and New South Wales Department of Environmental and Climate change.

Grace, M. R., D. P. Giling, S. Hladyz, V. Caron, R. M. Thompson, and R. Mac Nally. 2015. Fast processing of diel oxygen curves: Estimating stream metabolism with BASE (BAyesian Single- station Estimation). Limnol. Oceanogr. Meth. 13: 103-114.

Green, S. A., and N. B. Blough. 1994. Optical absorption and fluorescence properties of chromophoric dissolved organic matter in natural waters. Limnol. Oceanogr. 39:

1903–1916.

Grimm, N. B., and S. G. Fisher. 1986. Nitrogen limitation in a Sonoran Desert stream. J. N. Am. Benthol. Soc. 5: 2-15.

Grimm, N. B., and S. G. Fisher. 1989. Stability of periphyton and macroinvertebrates to disturbance by flash floods in a desert stream. J. N. Am. Benthol. Soc. 8: 293-307.

Hornberger, G. M., and M. G. Kelly. 1975. Atmospheric reaeration in a river using productivity analysis. J. Environ. Eng. Div. 101: 729–739.

Holgerson, M. A. 2015. Drivers of carbon dioxide and methane supersaturation in small, temporary ponds. Biogeochemistry 124: 305-318.

Holgerson, M. A., and P. A. Raymond. 2016. Large contribution to inland water $CO_2$ and $CH_4$ emissions from very small ponds. Nat. Geosci. 9: 222.

Hotchkiss, E. R., R. O. Hall Jr, R. A. Sponseller, D. Butman, J. Klaminder, H. Laudon, ... and J. Karlsson. 2015. Sources of and processes controlling $CO_2$ emissions change with the size of streams and rivers. Nat. Geosci. 8: 696.

Humphries, P., H. Keckeis, and B. Finlayson. 2014. The river wave concept: integrating river ecosystem models. BioScience 64: 870-882.

Iles, J. 2019. Nutrient limitation and interactions with organic matter and sediments within dryland streams of the Pilbara region of northwest Australia. Dissertation, The University of Western Australia.

Jähne, B., O. Münnich, R. Bösinger, A. Dutzi, W. Huber, and P. Libner. 1987. On the parameters influencing air-water gas exchange. J. Geophys. Res. 92:1937-1949.

Jones, J. B., Jr., S. G. Fisher, and N. B. Grimm. 1995. Vertical hydrologic exchange and ecosystem metabolism in a Sonoran Desert stream. Ecology 76: 942-952.

Jones, J. B. 2002. Groundwater controls on nutrient cycling in a Mojave Desert stream. Freshwater Biol. 47: 971-983.

Karlsson, J., P. Bystrom, J. Ask, P. Ask, L. Persson, and M. Jansson. 2009. Light limitation of nutrient-poor lake ecosystems. Nature 460: 506-509.

Keeling, R. F., S. C. Piper, A. F. Bollenbacher, and S. J. Walker. 2010. Monthly atmospheric $^{13}C/^{12}C$ isotopic ratios for 11 SIO stations. In Trends: A Compendium of Data on Global Change. U.S. Department of Energy.

Kufel, L., and I. Kufel. 2002. Chara beds acting as nutrient sinks in shallow lakes—a review. Aquat. Bot. 72: 249-260.

Lake, P. S. 2003. Ecological effects of perturbation by drought in flowing waters. Freshwater Biol. 48: 1161-1172.

Larned, S. T., T. Datry, D. B. Arscott, and K. Tockner. 2010. Emerging concepts in temporary-river ecology. Freshwater Biol. 55: 717-738.

Marlier, J. F., and M. H. O'Leary. 1984. Carbon kinetic isotope effects on the hydration of carbon dioxide and the dehydration of bicarbonate ion. J. Am. Chem. Soc. 106: 5054–5057.

McConnaughey, T. 1998. Acid secretion, calcification, and photosynthetic carbon concentrating mechanisms. Can. J. Bot. 76: 1119–1126.

McCutchan, J. H., W. M. Lewis, and J. F. Saunders. 1998. Uncertainty in the estimation of stream metabolism from open-channel oxygen concentrations. J. N. Am. Benthol. Soc. 17: 155-164.

McKnight, D. M., E. W. Boyer, P. K. Westerhoff, P. T. Doran, T. Kulbe, and D. T. Andersen. 2001. Spectrofluorometric characterization of dissolved organic matter for indication of precursor organic material and aromaticity. Limnol. Oceanogr. 46: 38-48.

Mulholland, P. J., A. D. Steinman, A. V. Palumbo, J. W. Elwood, and D. B. Kirschtel. 1991. Role of nutrient cycling and herbivory in regulating periphyton communities in laboratory streams. Ecology 72: 966-982.

Mulholland, P. J., E. R. Marzolf, S. P. Hendricks, R. V. Wilkerson, and A. K. Baybayan. 1995. Longitudinal patterns of nutrient cycling and periphyton characteristics in streams: A test of upstream-downstream linkage. J. N. Am. Benthol. Soc. 14: 357-370.

Mulholland, P. J., C. S. Fellows, J. L. Tank, N. B. Grimm, J. R. Webster, S. K. Hamilton, E. Martí, L. Ashkenas, W. B. Bowden, W. K. Dodds, and W. H. McDowell. 2001. Inter- biome comparison of factors controlling stream metabolism. Freshwater Biol. 46: 1503-1517.

Murphy, J., and J. P. Riley. 1962. A modified single solution method for the determination of phosphate in natural waters. Anal. Chim. Acta 27: 31-36.

Nimick, D. A., C. H. Gammons, and S. R. Parker. 2011. Diel biogeochemical processes and their effect on the aqueous chemistry of streams: A review. Chem. Geol. 283: 3-17.

Odum, H. T. 1956. Primary Production in Flowing Waters. Limnol. Oceanogr. 1: 102-117.

Oliver, R. L., and C. J. Merrick. 2006. Partitioning of river metabolism identifies phytoplankton as a major contributor in the regulated Murray River (Australia). Freshwater Biol 51: 1131-1148.

Parker, S. R., S. R. Poulson, C. H. Gammons, and M. D. Degrandpre. 2005. Biogeochemical controls on diel cycling of stable isotopes of dissolved O2 and dissolved inorganic carbon in the Big Hole River, Montana. Environ. Sci. Technol. 39: 7134-7140.

Parker, S. R., C. H. Gammons, S. R. Poulson, M. D. Degrandpre, C. L. Weyer, M. G. Smith, J. N. Babcock, and Y. Oba. 2010. Diel behavior of stable isotopes of dissolved oxygen and dissolved inorganic carbon in rivers over a range of trophic conditions, and in a mesocosm experiment. Chem. Geol. 269: 22-32.

Pinardi, M., M. Bartoli, D. Longhi, and P. Viaroli, P. 2011. Net autotrophy in a fluvial lake: the relative role of phytoplankton and floating-leaved macrophytes. Aquat. Sci. 73:

389-403.

Pronin, E., Pełechaty, M., Apolinarska, K., Pukacz, A., & Frankowski, M. 2016. Sharp differences in the $\delta^{13}C$ values of organic matter and carbonate encrustations but not in ambient water DIC between two morphologically distinct charophytes. Hydrobiologia 773: 177-191.

R Core Team. 2017. R: A language and environment for statistical computing. R Foundation for Statistical Computing.

Rasmussen, J. J., A. Baattrup-Pedersen, T. Riis, and N. Friberg. 2011. Stream ecosystem properties and processes along a temperature gradient. Aquat. Ecol. 45: 231-242.

Rouder, J. N. and R. D. Morey. 2013. Default Bayes Factors for Model Selection in Regression. Multivariate Behav. Res. 47: 877-903.

Rouillard A., Skrzypek G, Dogramaci S, Turney C, Grierson PF, 2015. Impacts of high inter-annual variability of rainfall on a century of extreme hydrological regime of northwest Australia. Hydrol. Earth Syst. Sci. 19: 2057-2078.

Scott, J. T., J. A. Back, J. M. Taylor, and R. S. King. 2008. Does nutrient enrichment decouple algal–bacterial production in periphyton? J. N. Am. Benthol. Soc. 27: 332-344.

Siebers, A. R., N. E. Pettit, G. Skrzypek, J. B. Fellman, S. Dogramaci, and P. F. Grierson. 2016. Alluvial ground water influences dissolved organic matter biogeochemistry of pools within intermittent dryland streams. Freshwater Biol. 61: 1228-1241.

Skrzypek, G. 2013. Normalization procedures and reference material selection in stable HCNOS isotope analyses: an overview. Anal. Bioanal. Chem. 405: 2815-2823.

Skrzypek, G., S. Dogramaci, and P. F. Grierson. 2013. Geochemical and hydrological processes controlling groundwater salinity of a large inland wetland of northwest Australia. Chem. Geo. 357: 164-177.

Smith, S. V. 1985. Physical, chemical and biological characteristics of $CO_2$ gas flux across the air-water interface. Plant Cell Environ. 8:387-398.

Sobek, S., L. J. Tranvik, and J. J. Cole. 2005. Temperature independence of carbon dioxide supersaturation in global lakes. Global Biogeochem. Cycles 19: GB2003, doi:10.1029/2004GB002264.

Staehr, P. A., D. Bade, M. C. Van de Bogert, G. R. Koch, C. Williamson, P. Hanson, J. J. Cole, and T. Kratz. 2010. Lake metabolism and the diel oxygen technique: State of the science. Limnol. Oceanogr. Methods 8: 628-644.

Stanley, E. H., S. G. Fisher, and N. B. Grimm. 1997. Ecosystem expansion and contraction in streams. BioScience 47: 427-435.

Tank, J. L., E. Martí, T. Riis, D. von Schiller, A. J. Reisinger, W. K. Dodds, M. R. Whiles, L. R. Ashkenas, and others. 2017. Partitioning assimilatory nitrogen uptake in streams: an analysis of stable isotope tracer additions across continents. Ecol. Monograph. doi:10.1002/ecm.1280.

Tobias, C. R., J. K. Böhlke, and W. H. Judson. 2007. The oxygen-18 isotope approach for measuring aquatic metabolism in high-productivity waters. Limnol. Oceanogr. 52: 1439-1453.

Tobias, C., and J. K. Böhlke. 2011. Biological and geochemical controls on diel dissolved inorganic carbon cycling in a low-order agricultural stream: Implications for reach scales and beyond. Chem. Geol. 283: 18-30.

Townsend, S. A., I. T. Webster, and J. H. Schult. 2011. Metabolism in a groundwater-fed river system in the Australian wet/dry tropics: tight coupling of photosynthesis and respiration. J. N. Am. Benthol. Soc. 30: 603-620.

Valett, H. M., S. G. Fisher, N. B. Grimm, and P. Camill. 1994. Vertical hydrologic exchange and ecological stability of a desert stream ecosystem. Ecology 75: 548-560.

Valett, H. M., J. A. Morrice, C. N. Dahm, and M. E. Campana. 1996. Parent lithology, surface–groundwater exchange, and nitrate retention in headwater streams. Limnol. Oceanogr. 41: 333-345.

Vazquez, E., S. Amalfitano, S. Fazi, and A. Butturini. 2011. Dissolved organic matter composition in a fragmented mediterranean fluvial system under severe drought conditions. Biogeochemistry 102: 59-72.

von Schiller, D., S. Bernal, C. N. Dahm, and E. Martí. 2017. Nutrient and organic matter dynamics in intermittent rivers and ephemeral streams. In: Datry, T., N. Bonada, and A. J. Boulton (eds) Intermittent rivers and ephemeral streams. Academic Press, pp 135-160.

Wanninkhof, R. 1992. Relationship between wind speed and gas exchange over the ocean. J. Geophys. Res. 97:7373-7382.

Water Environmental Federation (WEF) & American Public Health Association (APHA). 2005. Standard methods for the examination of water and wastewater. American Public Health Association (APHA): Washington, DC, USA.

Webster, I. T., N. Rea, A. V. Padovan, P. Dostine, S. A. Townsend, and S. Cook. 2005. An analysis of primary production in the Daly River, a relatively unimpacted tropical river in northern Australia. Mar. Freshw. Res. 56: 303-316.

Wiegner, T. N., L. A. Kaplan, J. D. Newbold, and P. H. Ostrom. 2005. Contribution of dissolved organic C to stream metabolism: a mesocosm study using $^{13}$C-enriched tree-tissue leachate. J. N. Am. Benthol. Soc. 24: 48-67.

Table 1: Physical and chemical characteristics of pools in Coondiner Creek (CND1, 3, 4) and Ben's Oasis (BO3, 4) at samplings in October and November 2012. $\delta^{13}C_{DIC}$ values, water temperature, and dissolved oxygen (DO) are summarised as ranges (min. to max.) due to significant diel variation. – indicates measurements were not taken within the pool. * indicates all concentrations were below detection limits.

| Parameter | Pool | | | | |
|---|---|---|---|---|---|
| | CND1 | CND3 | CND4 | BO3 | BO4 |
| Pool size ($m^2$) | 192.0 | 38.8 | 21.5 | 1352.0 | 173.0 |
| Pool aquatic vegetation area ($m^2$) | 66.7 | 5.9 | 0.0 | 135.2 | 69.2 |
| Pool aquatic vegetation cover (%) | 34.7 | 15.3 | 0.0 | 10.0 | 40.0 |
| Average depth (m) | 0.18 | 0.14 | 0.10 | 0.84 | 0.16 |
| $\delta^{18}O$ (‰) | -6.49 | -1.85 | 13.10 | -3.05 | -7.14 |
| $\delta^{2}H$ (‰) | -47.32 | -27.27 | 34.94 | -18.70 | -51.30 |
| $\delta^{13}C_{DIC}$ (‰) | - | -10.86 to -9.96 | - | -12.80 to -12.16 | - |

| | | | | | |
|---|---|---|---|---|---|
| Temperature ($^0$C) | 22.0 to 29.5 | 20.3 to 26.3 | 17.3 to 26.3 | 23.3 to 27.0 | 21.0 to 25.6 |
| DO (mg $L^{-1}$) | 0.5 to 7.8 | 0.9 to 4.4 | 0.0 to 8.0 | 0.1 to 1.4 | 1.1 to 4.6 |
| pH | 7.8 | 7.6 | 7.7 | 7.9 | 8.0 |
| FI | 1.43 | 1.56 | 1.68 | 1.36 | 1.36 |
| DIN (mg $L^{-1}$) | 0.11 | 0.06 | 0.07 | 0.05 | 0.05 |
| SRP (µg $L^{-1}$) | < 2.5* | < 2.5* | < 2.5* | < 2.5* | < 2.5* |

790

Table 2: Estimates of ecosystem metabolism within pools of Coondiner Creek (CND1, 3, 4) and Ben's Oasis (BO3, 4) at samplings in October and November 2012. Original units of estimation (mg $O_2$ $L^{-1}$ $d^{-1}$) are given as means and standard deviations (±) of posterior distributions. Areal rates (g $O_2$ or C $m^{-2}$ $d^{-2}$) are subsequently derived from posterior distribution means (for conversion equations, see Methods: Modelling of ecosystem metabolism). Posterior estimates are also given for modelled re-aeration flux (*k*), temperature dependence of respiration (Θ) and light saturation of photosynthesis (*p*).

| Units | Parameter | Pool | | | | |
|---|---|---|---|---|---|---|
| | | CND1 | CND3 | CND4 | BO3 | BO4 |
| mg $O_2$ $L^{-1}$ $d^{-1}$ | GPP | 9.63 ± 0.23 | 3.75 ± 0.30 | 10.73 ± 0.68 | 1.25 ± 0.04 | 2.18 ± 0.09 |
| | ER | 10.98 ± 0.21 | 6.12 ± 0.28 | 11.95 ± 0.87 | 3.14 ± 0.31 | 3.03 ± 0.34 |
| | GPP:ER | 0.88 | 0.61 | 0.90 | 0.40 | 0.72 |
| g $O_2$ $m^{-2}$ $d^{-1}$ | GPP | 1.73 | 0.52 | 1.07 | 1.05 | 0.35 |
| | ER | 1.98 | 0.86 | 1.19 | 2.64 | 0.49 |
| g C $m^{-2}$ $d^{-1}$ | GPP | 0.54 | 0.16 | 0.34 | 0.33 | 0.11 |

| | | | | | |
|---|---|---|---|---|---|
| ER | 0.63 | 0.27 | 0.38 | 0.84 | 0.15 |
| $k$ (m $d^{-1}$) | 0.78 ± 0.04 | 0.39 ± 0.04 | 0.30 ± 0.06 | 0.25 ± 0.04 | 0.18 ± 0.05 |
| Θ | 1.3 ± 0.001 | 1.29 ± 0.01 | 1.12 ± 0.01 | 1.0 ± 0.001 | 1.0 ± 0.001 |
| $p$ | 0.30 ± 0.001 | 0.51 ± 0.09 | 0.37 ± 0.04 | 0.31 ± 0.01 | 0.79 ± 0.11 |

796

**Figure captions**

Figure 1: Location of the study pools along a) Coondiner Creek (CND 1-7) and b) Ben's Oasis (BO1-4) in northwest Australia.

Figure 2: Diel variation in a) $\delta^{13}C_{DIC}$ values, c) water temperature and e) dissolved oxygen (DO) saturation in Coondiner Creek pool 3 (CND3; white dots). Diel variation in b) $\delta^{13}C_{DIC}$ values, d) water temperature and f) DO saturation in Ben's Oasis pool 3 (BO3; black dots). Shaded areas represent night-time measurements (c. 18:05 – 05:20). Generalised additive model (GAM) fitted values are shown by solid lines. Dashed lines indicate 95% confidence limits for fitted values. Axis scales are kept equivalent for comparisons except in the case of $\delta^{13}C_{DIC}$, where absolute y-axis values differ but the range is equal (1.2 ‰).

Figure 3: Relationships between a) $\delta^{13}C_{DIC}$ values and temperature in Coondiner Creek pool 3 (CND3) ,and b) change in $\delta^{13}C_{DIC}$ values between consecutive time periods ($\Delta^{13}C_{t2\text{-}t1}$) and rates of change in temperature ($\Delta T_{t2\text{-}t1}$) in CND3. Generalised linear model (GLM) fitted values are shown by solid lines. Dashed lines indicate 95% confidence limits for fitted values.

Figure 4: Perspective plot of generalised linear model (GLM) predictions for a) $\delta^{13}C_{DIC}$ values relative to temperature and photosynthetically active radiation (PAR) in Ben's Oasis pool 3 (BO3), and b) change in $\delta^{13}C_{DIC}$ values between consecutive time periods ($\Delta^{13}C_{t2\text{-}t1}$) relative to rates of change in temperature ($\Delta T_{t2\text{-}t1}$) and rates of change in PAR ($\Delta PAR_{t2\text{-}t1}$) in BO3. Original data points and residuals relative to GLM fit are also shown.

Figure 5: Partial residual plots for generalised linear models (GLMs) explaining gross primary productivity (GPP) rates as a function of a) pool area, b) pool aquatic vegetation cover, and c) FI values; ecosystem respiration (ER) rates as a function of d) GPP, e) pool aquatic vegetation cover, and f) FI values; and GPP:ER ratios as a function of g) pool aquatic

vegetation area, h) pool aquatic vegetation cover, and i) FI values. Bands show confidence intervals for fitted terms.

Figure 1

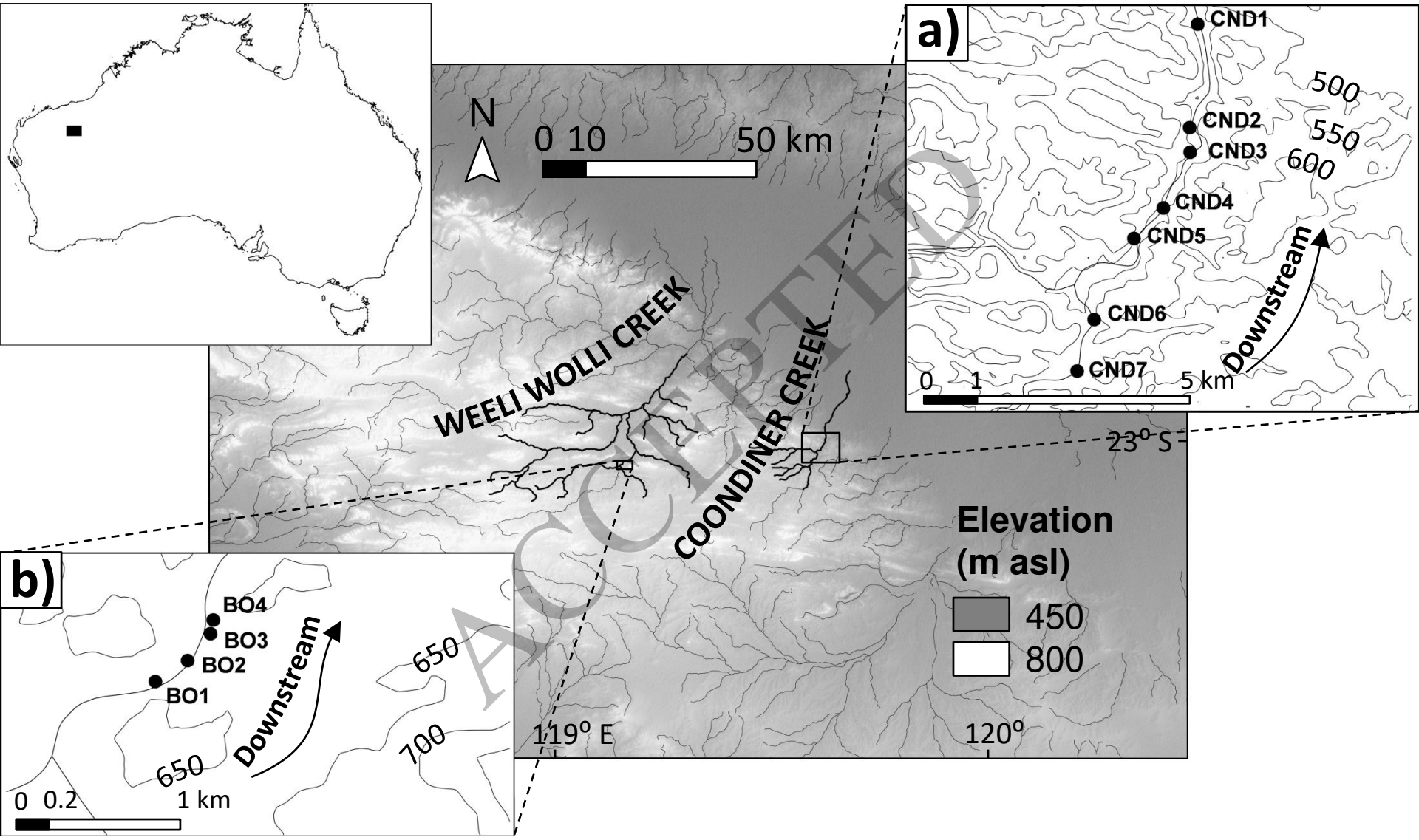

Figure 2

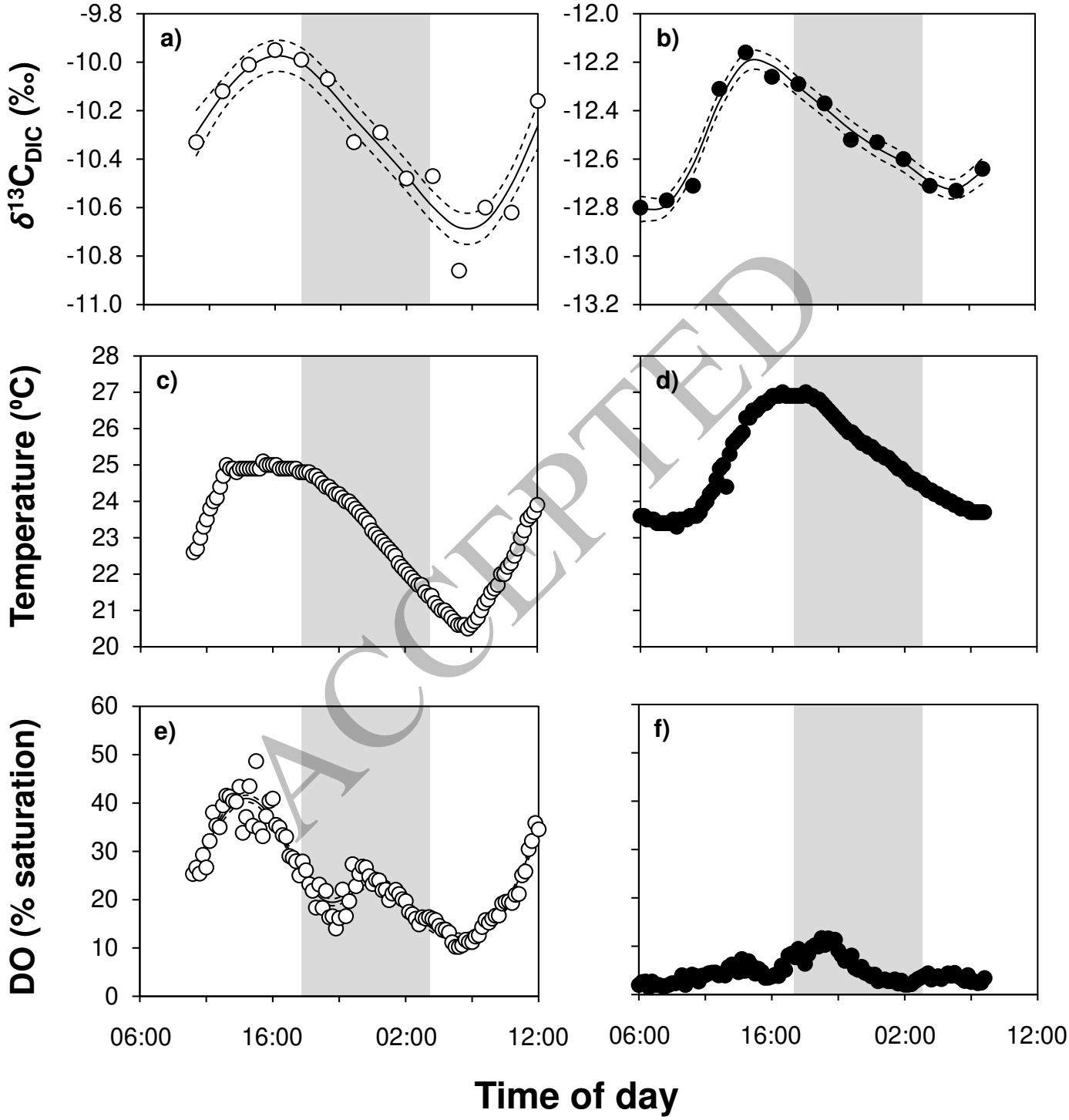

Figure 3

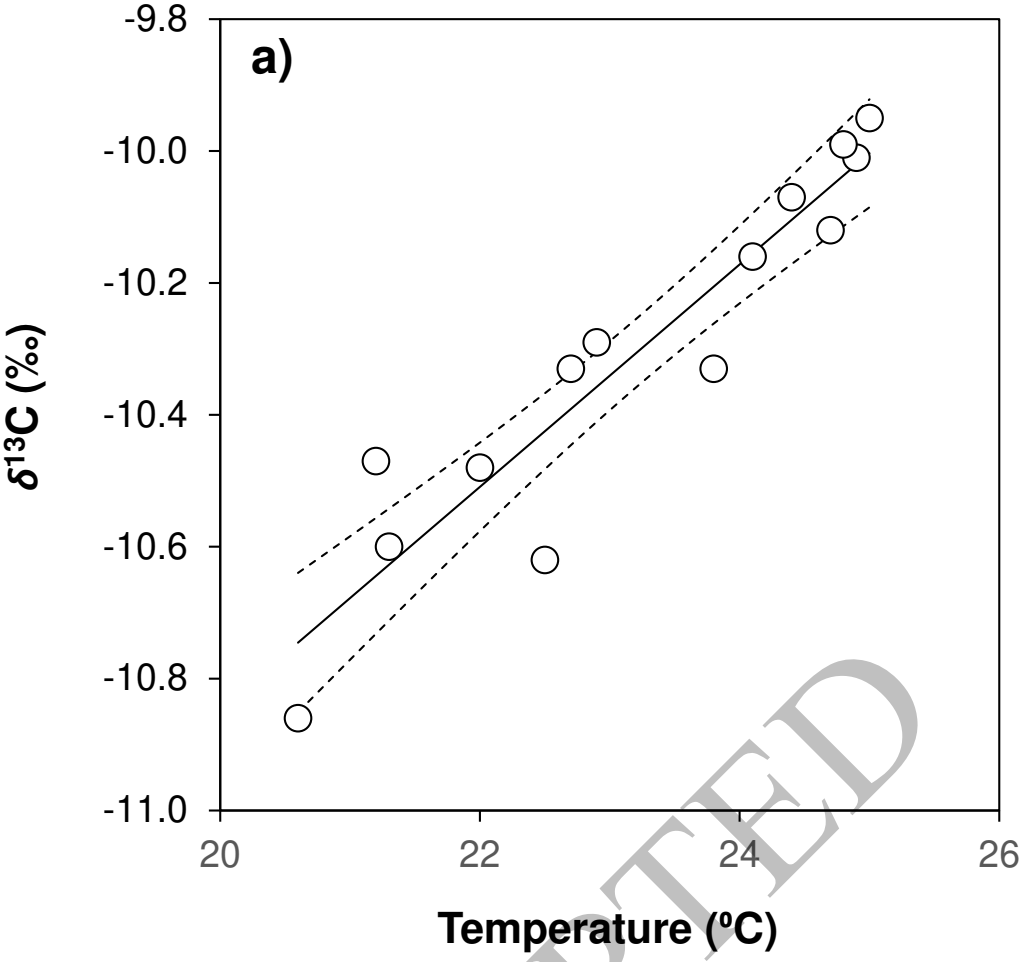


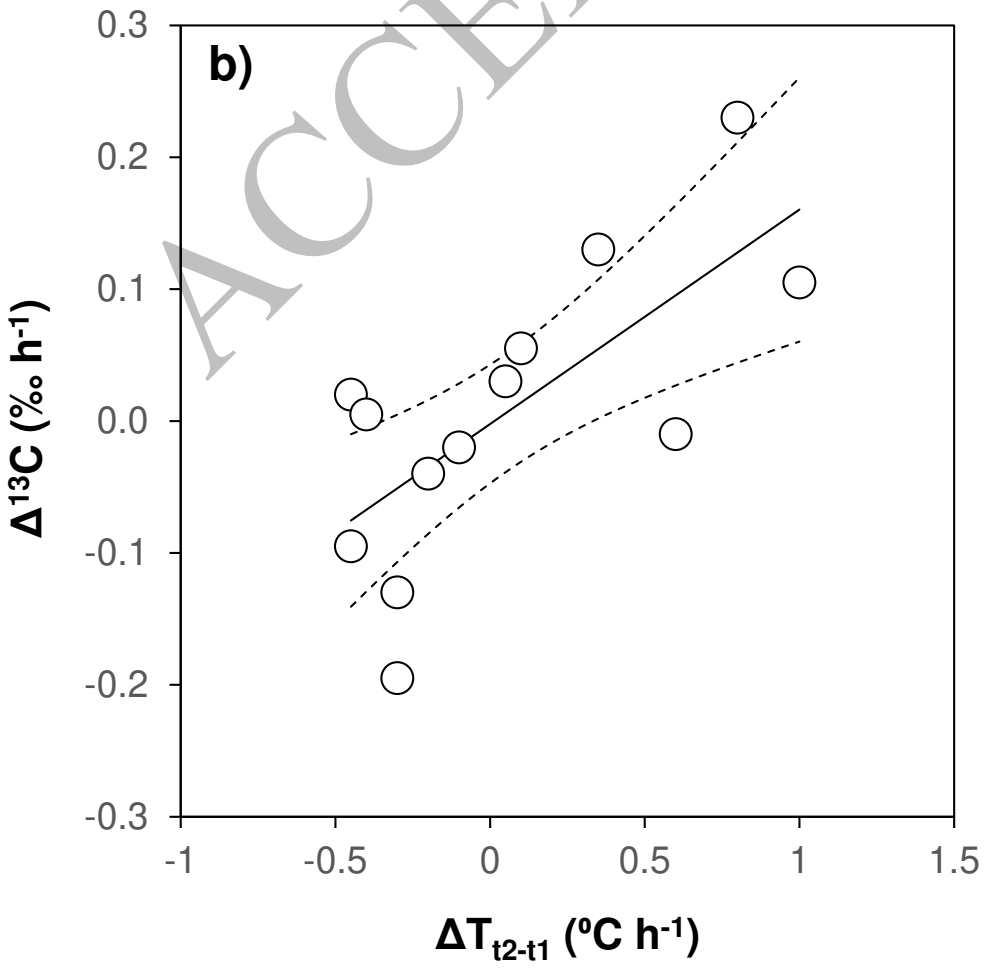

Figure 4

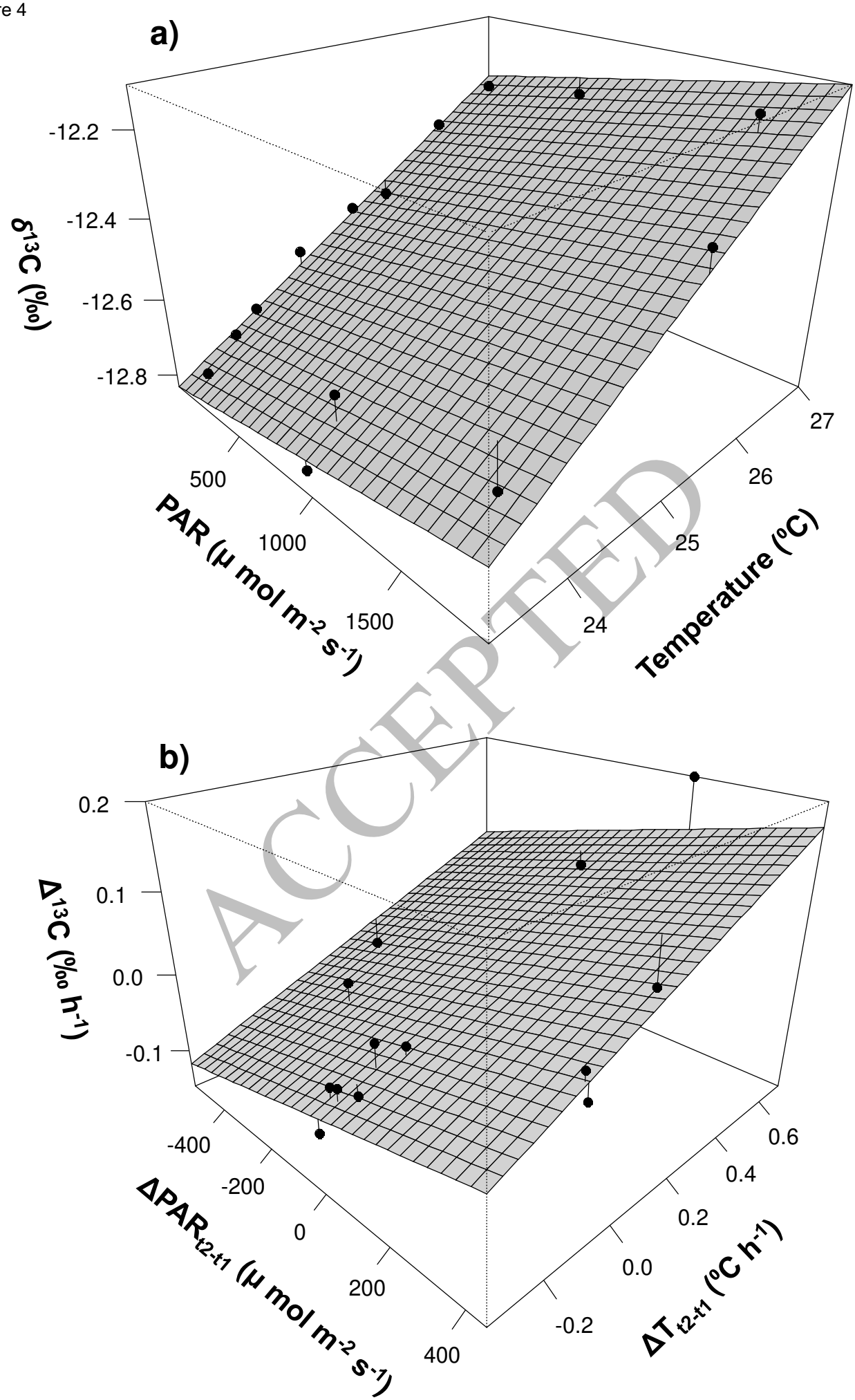

Figure 5

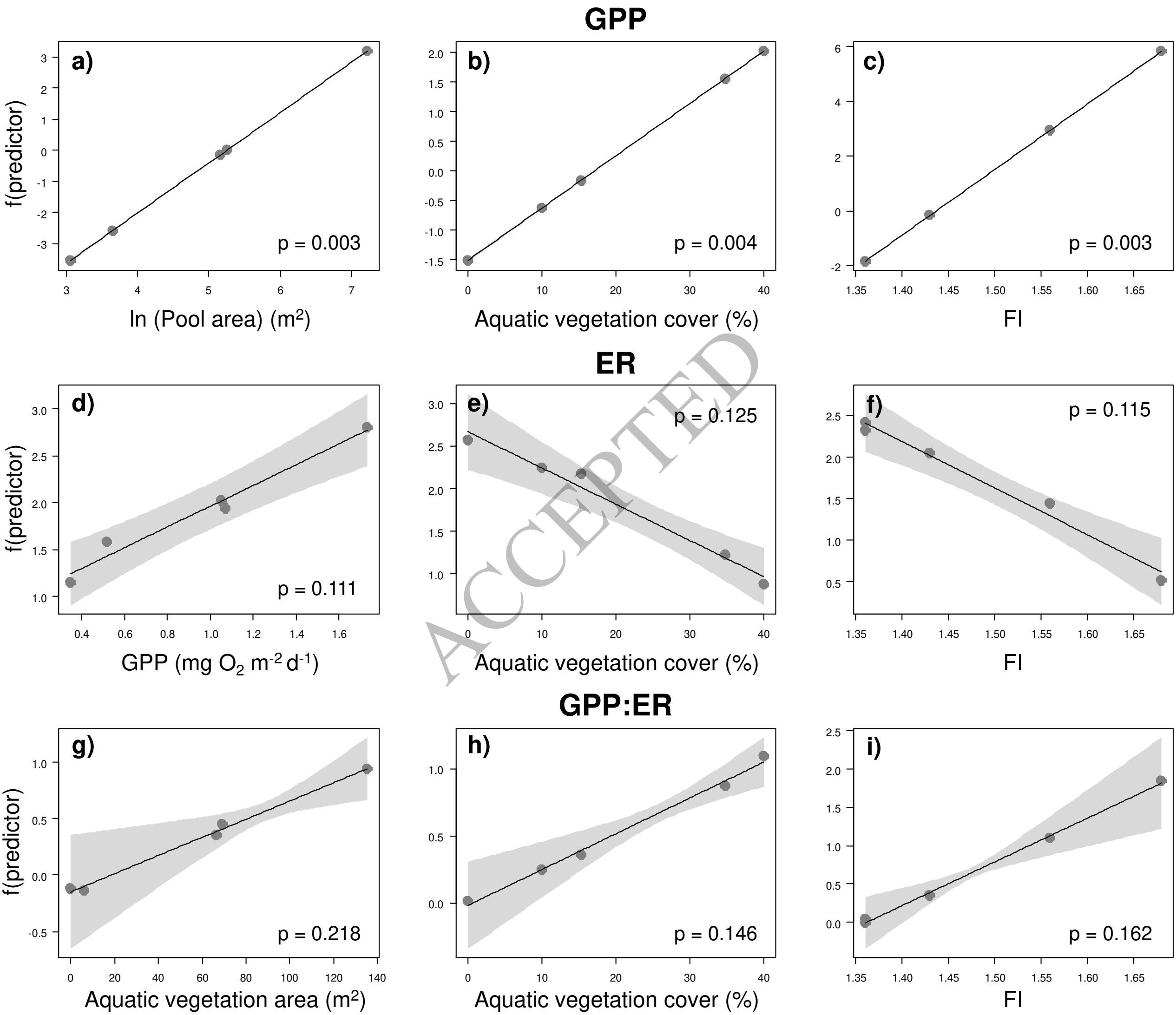

## Supplementary material

Figure A.1: Relationship between $\delta^{18}O$ and $\delta^{2}H$ values for alluvial ground water (AW) and pool water samples collected in October 2012 from Coondiner Creek, and November 2012 from Weeli Wolli Creek (Ben's Oasis). The local meteoric water line (LMWL) and local evaporation line (LEL) for the Hamersley Basin are taken from Dogramaci et al. (2012). Alluvial ground water $\delta^{18}O$ and $\delta^{2}H$ values are taken from Siebers et al. (2016) (measured between May 2011 and July 2012). See text for pool abbreviations.

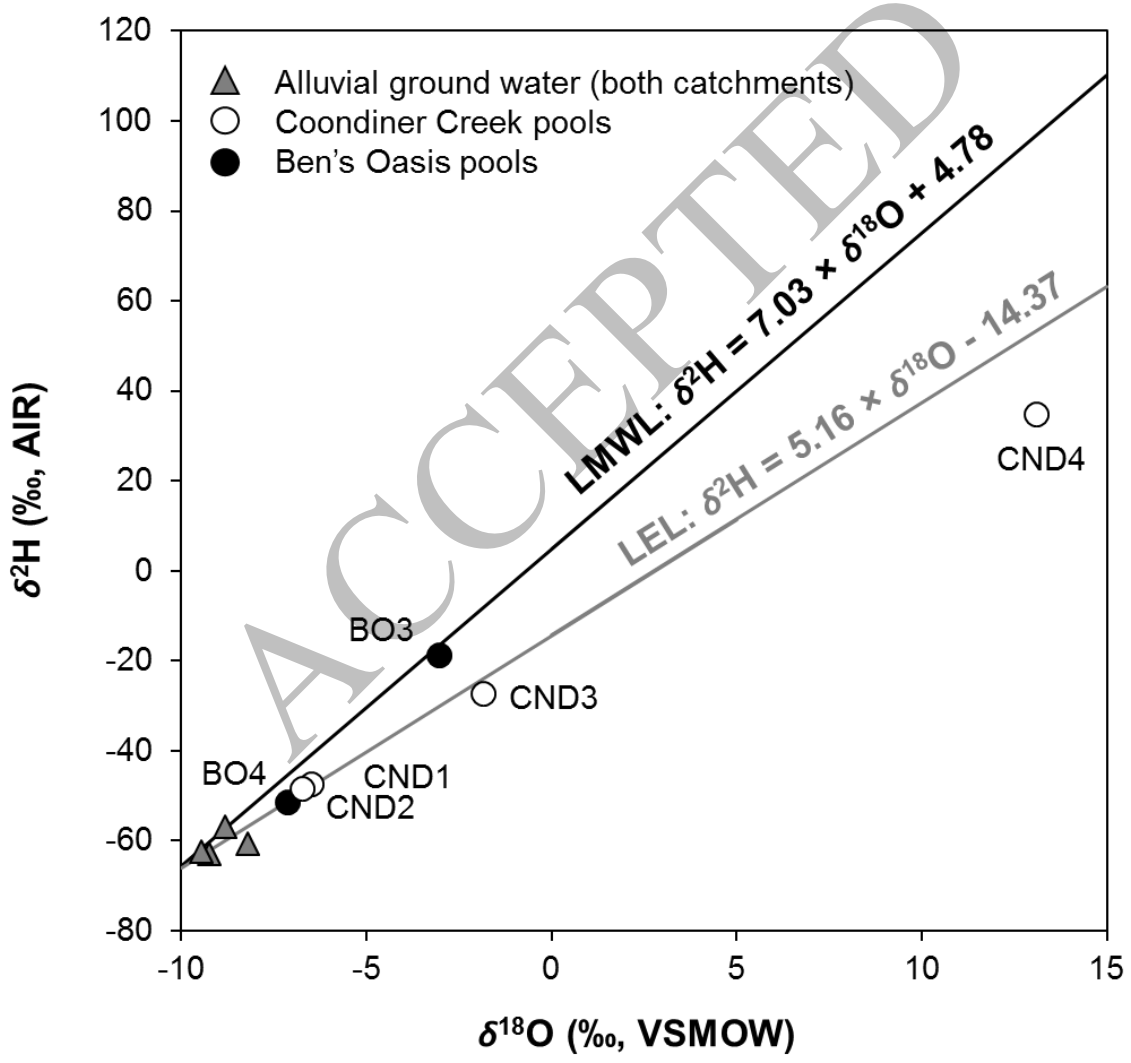

Table A.1: Diel measurements of chemical and physical parameters in Coondiner Creek pool 3 (CND3) and Ben's Oasis pool 3 (BO3).

| Pool | Time | $\delta^{13}C_{DIC}$ (‰) | Temperature (° C) | DO (% saturation) | $\delta^{18}O$ (‰) | PAR (µ mol $m^{-2}$ $s^{-1}$) | DIN (mg $L^{-1}$) |
|---|---|---|---|---|---|---|---|
| CND3 | 10:00 | -10.33 | 22.7 | 25.3 | -1.78 | 1711.2 | 0.050 |
| | 12:00 | -10.12 | 24.7 | 35.0 | -1.84 | 1938.7 | 0.049 |
| | 14:00 | -10.01 | 24.9 | 37.1 | -1.67 | 1888.7 | 0.058 |
| | 16:00 | -9.95 | 25.0 | 40.9 | -1.81 | 981.2 | 0.068 |
| | 18:00 | -9.99 | 24.8 | 25.0 | -1.65 | 33.7 | 0.062 |
| | 20:00 | -10.07 | 24.4 | 21.9 | -1.70 | 1.2 | 0.217 |
| | 22:00 | -10.33 | 23.8 | 27.3 | -1.58 | 1.2 | 0.127 |
| | 00:00 | -10.29 | 22.9 | 24.0 | -1.63 | 1.2 | 0.042 |
| | 02:00 | -10.48 | 22.0 | 19.7 | -1.77 | 1.2 | 0.015 |
| | 04:00 | -10.47 | 21.2 | 16.1 | -1.67 | 1.2 | 0.041 |
| | 06:00 | -10.86 | 20.6 | 10.2 | -1.83 | 41.2 | 0.015 |
| | 08:00 | -10.60 | 21.3 | 15.8 | -1.73 | 703.7 | 0.024 |
| | 10:00 | -10.62 | 22.5 | 19.3 | -1.71 | 1366.2 | 0.019 |
| | 12:00 | -10.16 | 24.1 | 34.6 | -1.55 | 1581.2 | 0.036 |

| | | | | | | | |
|---|---|---|---|---|---|---|---|
| BO3 | 06:00 | -12.80 | 23.5 | 2.0 | -3.20 | 81.2 | 0.022 |
| | 08:00 | -12.77 | 23.3 | 1.8 | -3.04 | 983.7 | 0.048 |
| | 10:00 | -12.71 | 23.9 | 4.1 | -2.98 | 1633.7 | 0.028 |
| | 12:00 | -12.31 | 25.3 | 4.0 | -2.87 | 1903.7 | 0.050 |
| | 14:00 | -12.16 | 26.5 | 4.9 | -3.13 | 1686.2 | 0.090 |
| | 16:00 | -12.26 | 27.0 | 3.7 | -3.23 | 611.2 | 0.033 |
| | 18:00 | -12.29 | 26.9 | 9.5 | -3.27 | 51.2 | 0.027 |
| | 20:00 | -12.37 | 26.3 | 10.3 | -3.31 | 1.2 | 0.040 |
| | 22:00 | -12.52 | 25.6 | 8.1 | -3.14 | 1.2 | 0.028 |
| | 00:00 | -12.53 | 25.2 | 2.8 | -2.89 | 1.2 | 0.032 |
| | 02:00 | -12.60 | 24.6 | 2.0 | -3.08 | 1.2 | 0.033 |
| | 04:00 | -12.71 | 24.1 | 3.1 | -3.32 | 1.2 | 0.087 |
| | 06:00 | -12.73 | 23.8 | 3.8 | -3.31 | 78.7 | 0.034 |
| | 08:00 | -12.64 | 23.6 | 3.4 | -3.06 | 966.2 | 0.095 |

11

Figure A.2: Diel variation in $\delta^2$H values in Coondiner Creek pool 3 (CND3). Shaded areas represent night-time measurements (c. 18:05 – 05:20). Generalised additive model (GAM) fitted values are shown by solid lines. Dashed lines indicate 95 % confidence limits for fitted values.